J. Civil Eng. Mater.App. 2025 (September); 9(3): 131-144

Journal of Civil Engineering and Materials Application
Journal home page: http://jcema.com

Received: 16 July 2025 • Revised: 02 September 2025 • Accepted: 24 September 2025

Research

doi: 10.22034/jcema.2025.553798.1183

Parametric Nonlinear FEM Study of Load Transfer Efficiency in Jointed Plain Concrete Pavements

Goytom Gidey Desta [1*], Ashenafi Aregawi [2], Berhane Grum [2]

[1] Civil Engineering, Engineering and technology college, Adigrat University, Adigrat, Ethiopia
[2] School of Civil Engineering, Mekelle University, Mekelle, Ethiopia

*Correspondence should be addressed to Goytom Gidey Desta, Civil Engineering, Engineering and technology college, Adigrat University, Adigrat, Ethiopia
Email: gtekleee@gmail.com

ABSTRACT

This study develops a validated three-dimensional nonlinear finite element (FE) model in ABAQUS to evaluate the influence of key design parameters—slab thickness, dowel diameter, joint width, base modulus, axle load, and dowel–concrete interaction—on load transfer efficiency (LTE) in jointed plain concrete pavements (JPCPs). The model incorporates realistic dowel–concrete interface behavior, Concrete Damage Plasticity (CDP), and multilayer base–subgrade support.

Simulation results indicate that increasing slab thickness from 0.25 m to 0.35 m enhances LTE by 0.70 %, while enlarging dowel diameter from 32 mm to 38 mm increases LTE by 2.56 %. Conversely, widening the joint from 8–12 mm reduces LTE by 1.24 %. Base stiffness exhibits the strongest influence; increasing base modulus from 100 MPa to 10 000 MPa raises LTE by approximately 13.5 %. Heavier axle loads (8–15 tons) decrease LTE by about 4.12 %. Dowel–concrete friction and dowel support modulus have minimal effects (less than 1 %), indicating their limited contribution under typical design conditions.

The results indicate that LTE is primarily governed by loading, slab geometry, and base stiffness, whereas interface friction and dowel support modulus have only marginal effects. The validated model demonstrates strong agreement with analytical predictions (deviation <2.5 %), ensuring reliability for mechanistic pavement design applications.

Keywords: Load Transfer Efficiency (LTE); Jointed Plain Concrete Pavement (JPCP); Finite Element Method (FEM); Dowel–Concrete Interaction

Copyright © 2025, Goytom Gidey Desta. This is an open access paper distributed under the Creative Commons Attribution License,Journal of Civil Engineering and Materials Applicationis published by {ISNet}; Journal p-ISSN 2676-332X; Journal e-ISSN 2588-2880.

1. INTRODUCTION

Jointed Plain Concrete Pavements (JPCPs) are widely used in highway systems due to their durability and load-bearing capacity [1,2]. The performance of JPCPs depends on efficient load transfer across transverse joints, which control cracking and accommodate thermal and moisture-induced movements [3,4]. Inadequate load transfer leads to differential slab deflections, resulting in

distresses such as faulting, corner cracking, and joint deterioration [5,6].

Transverse joints act as structural discontinuities that transfer loads between adjacent slabs through dowel action, aggregate interlock, and subbase support [7–9]. Aggregate interlock contributes significantly when joint openings remain narrow (<0.8 mm); however, its influence decreases rapidly as the joint widens [10,11]. Hence, dowel action becomes the dominant mechanism, with parameters such as dowel diameter, spacing, alignment, and subbase stiffness strongly influencing LTE and overall pavement performance [12,9].

Researchers have identified Load Transfer Efficiency (LTE) as a key indicator of the structural integrity and serviceability of JPCPs, providing valuable insight into joint performance and the effectiveness of design features aimed at optimizing pavement longevity and ride quality [7,8,13,14]. Achieving high LTE mitigates load-related distresses by reducing stress concentrations and limiting relative slab movement [7,8]. Field observations indicate that LTE values above 70% generally correspond to satisfactory pavement performance [9,13]. Foundational analytical studies, notably Friberg's shear-transfer theory [15], established the theoretical basis for LTE in doweled joints. These early models, grounded in classical elastic theory [16], assumed linear material behavior, idealized boundary conditions, and simplified dowel–concrete interaction. While suitable for early design applications, such simplifications limit predictive accuracy under modern traffic and environmental loading conditions [17,18]. Consequently, contemporary JPCPs subjected to heavier traffic loads and complex material–structural interactions have revealed the limitations of linear-elastic assumptions [19-21].

Recent investigations demonstrate that perfectly bonded or linear-elastic models fail to capture essential nonlinear behaviors such as dowel slip, interface separation, and stiffness degradation under repeated loading [12,15,16]. As a result, advanced nonlinear finite element (FE) frameworks have been developed to better simulate dowel–concrete contact, subbase interaction, and stress redistribution under realistic field conditions [17,22].

In summary, the performance of JPCPs is primarily governed by LTE across transverse joints, which depends on the interaction between dowels, concrete, and the subbase. The limitations of traditional analytical models emphasize the need for advanced nonlinear numerical methods capable of reproducing the multi-mechanism behavior observed in field pavements.

1.1 Numerical and Field Investigations of LTE

Three-dimensional nonlinear finite element modeling (FEM) has become a widely used tool for simulating realistic joint behavior in JPCPs. These models incorporate key mechanisms such as dowel–concrete interaction, progressive concrete damage, and heterogeneous support conditions [23–26]. Field and laboratory investigations confirm that doweled and hybrid-reinforced systems can achieve LTE values exceeding 90% [3,4]. FEM analyses have identified dowel placement, joint width, interface bonding, slab thickness, and base stiffness as the principal parameters influencing LTE [15,21,27].

Higher base stiffness (≥300–350 MPa) enhances LTE and reduces slab cracking [28,29], while the use of fiber-reinforced polymer (FRP) or stainless-steel dowels has been shown to improve long-term performance [3,4,30]. Furthermore, recent advances in displacement and vibration sensing technologies allow real-time LTE evaluation consistent with traditional field-testing methods [31].

Despite these advancements, commonly used FEM tools such as ANSYS, EverFE, and DIANA still rely on embedded-contact or linear-elastic assumptions originally developed for reinforced concrete rather than JPCPs [16,17]. These simplifications overlook critical nonlinear effects—such as dowel slip, bearing deformation, and progressive concrete damage—leading to systematic overestimation of LTE [12,32]. For instance, Zang et al [12] reported a 15–20% overprediction of LTE using linear models, while Zewdie et al. [15] observed a 25% reduction in dowel shear capacity when nonlinear interfaces were considered. Huang et al. [33] found that LTE decreased from 85% to 68% under a 40 kN load due to cracking, whereas Davids et al. [21] and Bilal et al. [38] demonstrated that dowel looseness and joint widening significantly reduce LTE. Collectively, these findings highlight the necessity of nonlinear, multi-mechanism modeling to more accurately replicate field performance.

1.2. Research Gap and Study Objectives

Although substantial progress has been made in understanding joint behavior, the accurate prediction

of LTE in JPCPs remains constrained by simplified dowel–concrete interface modeling, coarse meshing, and idealized boundary assumptions [39-41]. Classical and empirical design frameworks—such as those proposed by AASHTO and Huang [1,25]—typically employ linear-elastic or fully bonded assumptions that cannot reproduce the nonlinear load transfer and degradation observed in field conditions. Even modern FEM models often neglect localized slip, bearing deformation, and stiffness loss, thereby limiting their ability to predict actual pavement response [15–18, 42].

To address these limitations, the present study develops a nonlinear finite element framework in Abaqus, featuring explicit surface-to-surface contact between dowel and concrete, integration of the Concrete Damage Plasticity (CDP) model, and refined meshing strategies [6,43]. This modeling approach enables realistic simulation of dowel–concrete interaction, stress redistribution, and load transfer degradation. Validation against analytical and experimental benchmarks ensures the reliability and applicability of the developed framework.

A systematic parametric analysis is conducted to examine the effects of slab thickness, dowel diameter, joint width, and subgrade stiffness on LTE and stress distribution. The outcomes of this analysis provide mechanistic insight into doweled joint behavior and support the performance-based design of durable concrete pavements.

While the proposed model effectively captures nonlinear load transfer mechanisms, certain limitations remain. The analysis assumes static loading and uniform support, without explicitly considering thermal or moisture gradients. Field instrumentation was not incorporated, and validation relied on published datasets. Nevertheless, the developed framework establishes a robust mechanistic foundation for LTE evaluation and lays the groundwork for future studies incorporating environmental and dynamic effects.

2. MATERIALS AND METHODS

2.1 Material Properties

The 3D finite element (FE) model represents two concrete slabs separated by a transverse joint, with mid-depth dowels spaced at 300 mm. Concrete (f'c = 40 MPa; ft = 3.5 MPa) was simulated using the Concrete Damage Plasticity (CDP) model [16,18], while the base and subgrade layers were assumed linear elastic, consistent with common mechanistic modeling approaches [6,16]. Seven cylindrical dowels were symmetrically distributed across the joint at 300 mm center-to-center spacing. To balance computational efficiency with stress accuracy, a slab width of 2.1 m was adopted, reflecting the estimated 0.7 m stress penetration from a corner wheel load [16,44]. Base and subgrade layers extended 0.4 m beyond the slab on each side to ensure complete stress distribution. A 10 mm joint width was provided to accommodate thermal expansion and contraction. Each dowel was embedded halfway into the loaded slab, with the remaining half interacting frictionally or sliding relative to the adjacent slab, depending on the dowel–concrete interface behavior [6,16,45].

Concrete was modeled using the nonlinear CDP model to capture both tensile cracking and compressive plasticity [16, 36]. The CDP input parameters were defined as a dilation angle (φ) of 15°, an eccentricity of 0.1, a biaxial-to-uniaxial compressive-strength ratio (Fb/Fc) of 1.16, and a tensile-to-compressive meridian ratio (k) of 0.666, representing concrete behavior under combined stress conditions [16, 46]. These represent typical concrete behavior under combined stress conditions. General material properties for all pavement layers and dowels are summarized in Table 1. The base and subgrade layers were assumed isotropic and linear elastic [47], while dowels were modeled as thermo-elastic–plastic to account for pseudo-temperature effects [48].

Table 1. Material Property and Geometric Parameters
(a) Concrete Slab, Base, and Subgrade)

Component	Length (m)	Width (m)	Thickness (m)	Young's Modulus, Ec (MPa)	Poisson's Ratio	Density (kg/m³)	CTE (°C⁻¹)
Slab	4.6	2.1	0.25	29.7×10^3	0.19	2400	1.08×10^{-5}
Base	10.01	2.9	0.20	310	0.3	2100	—
Subgrade	10.01	2.9	0.25	30.3	0.4	2040	—

(b) Steel Dowel Bars)

Component	Length (m)	Diameter (m)	Yield Stress (MPa)	Young's Modulus, Ec (MPa)	Poisson's Ratio	Density (kg/m³)	CTE (°C⁻¹)
Dowel	0.5	0.032	345	200×10^3	0.3	7830	1.22×10^{-5}

Notes: CTE = Coefficient of Thermal Expansion. SI units are used.

Table 2. CDP Model Parameters for Concrete Compression and Tension
(a) Concrete Compression Behavior)

Stress (Pa)	Crushing Strain	Damage (dc)	Crushing Strain (for dc)
1.50×10^7	0.0000000000	0.0000000	0.0000000000
2.02×10^7	0.0000747307	0.0000000	0.0000747307
3.00×10^7	0.0000988479	0.0000000	0.0000988479
4.03×10^7	0.0001541230	0.0000000	0.0001541230
5.00×10^7	0.0007615380	0.0000000	0.0007615380
4.02×10^7	0.0025575590	0.1954020	0.0025575590
2.02×10^7	0.0056754310	0.5963820	0.0056754310
5.28×10^6	0.0117331190	0.8948650	0.0117331190

(b) Concrete Tension Behavior)

Stress (Pa)	Cracking Strain	Damage (d_t)	Cracking Strain (for d_t)
1.99893×10^6	0.0000000000	0.0000000	0.0000000000
2.84200×10^6	0.0000333300	0.0000000	0.0000333300
1.86981×10^6	0.0001604270	0.4064110	0.0001604270
8.62723×10^5	0.0002797630	0.6963500	0.0002797630
2.26254×10^5	0.0006845900	0.9203890	0.0006845900
5.65760×10^4	0.0010867300	0.9800930	0.0010867300

Note: These define nonlinear concrete response under compression and tension.

2.2. Loading Conditions

A standard single-axle dual-wheel (SADW) system with an 80 kN total load (two 20 kN wheels spaced 300 mm apart) was applied, positioning the outer wheel above the corner dowel and 10 mm from the joint edge [15, 49], as illustrated in Figure 1.

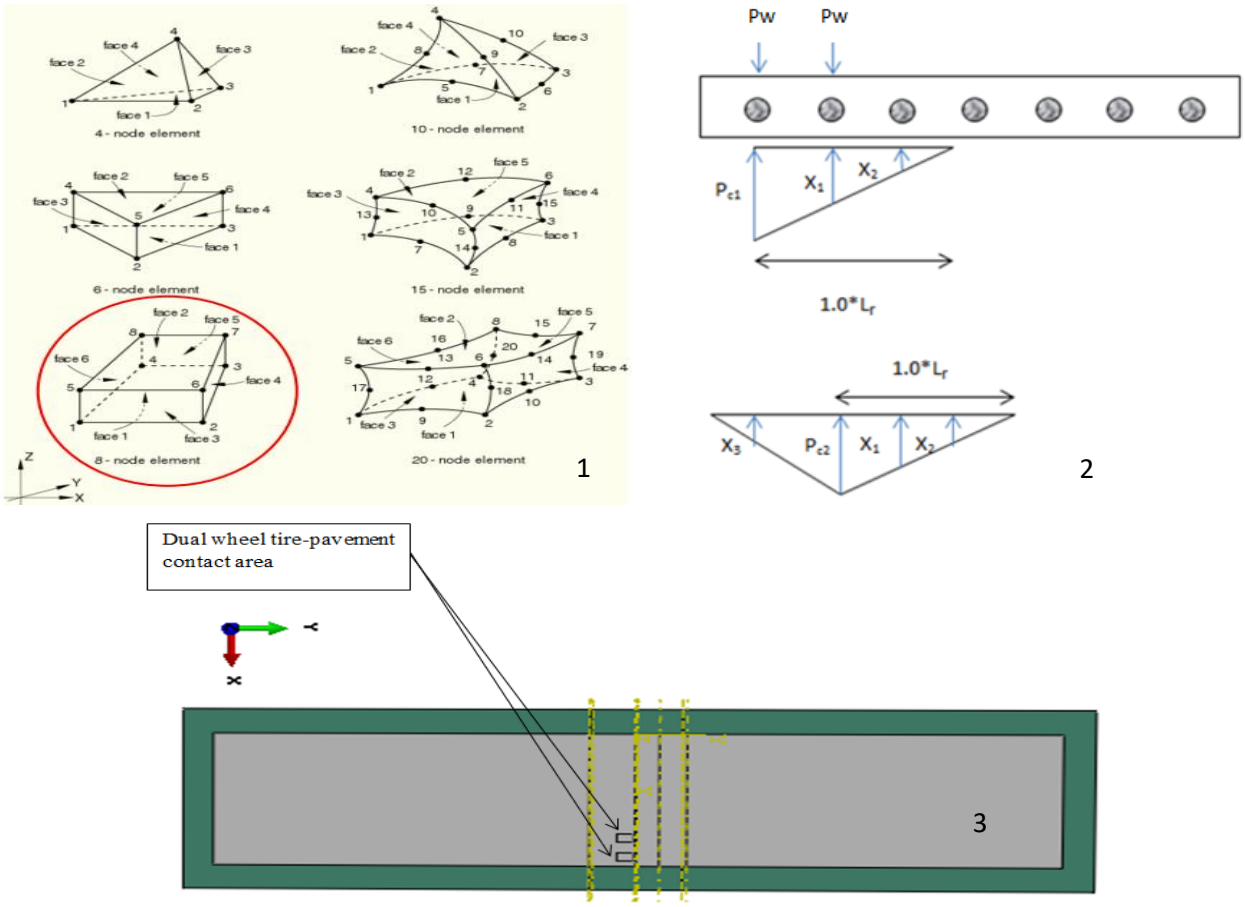

Figure 1. Abaqus solid elements (1) and corresponding load transfer distribution under dual-wheel loading (2). FE model representation of the rectangular loading area (3).

A uniform pressure of 830 kPa was applied over a rectangular contact area of 0.187 × 0.129 m to simulate realistic wheel–slab interaction [15, 30]. A minor pseudo-temperature increase (285–290 K) was introduced to induce initial contact pressure between dowels and concrete [50].

2.3 Finite Element Modeling

2.3.1 Element Type

A three-dimensional solid finite-element model was developed using first-order, reduced-integration C3D8R brick elements with hourglass control in ABAQUS [37]. Solid continuum elements were selected to capture complex stress and displacement fields more accurately than truss, beam, or shell elements [37]. Reduced integration minimized computational cost and mitigated volumetric or shear locking in bending-dominated regions [37].

2.3.2 Interface Modeling

The slab–base interface was modeled with hard contact and a friction coefficient of 0.95, while the base–subgrade interface was tied to enforce identical displacements [39]. A schematic of these contact interfaces is shown in Figure 2. Dowel–concrete interaction (DCI) was captured through two complementary mechanisms to realistically simulate load transfer across the joint [15, 51, 52].

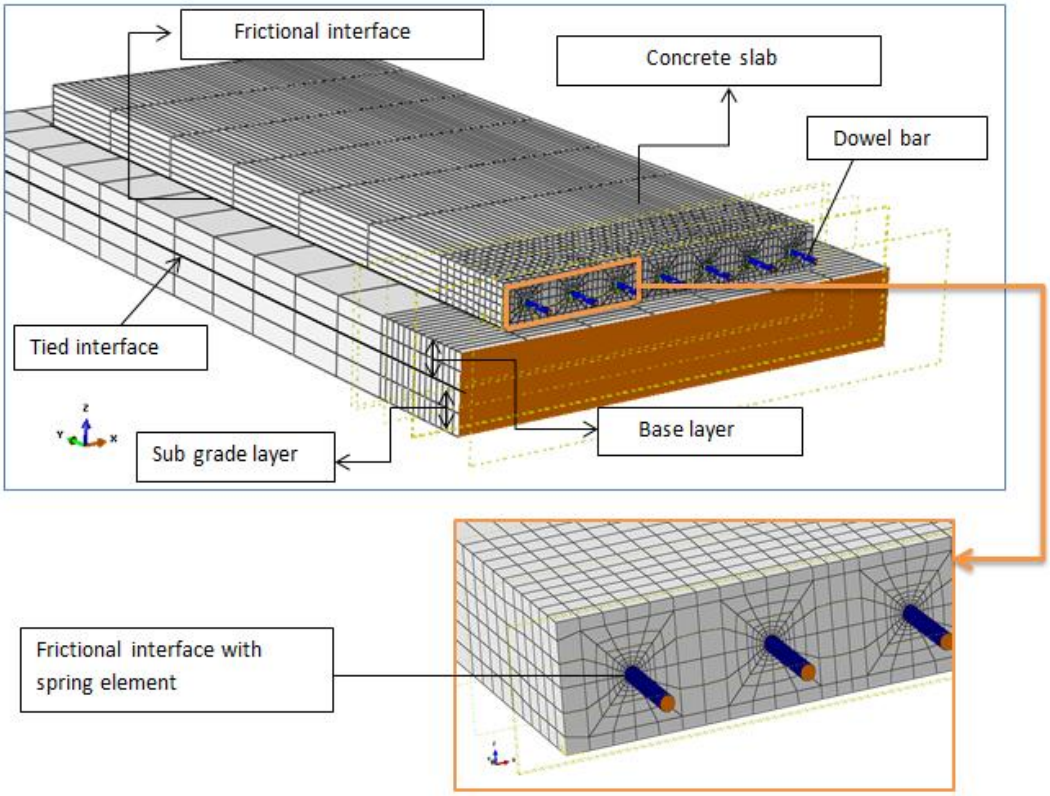

Figure 2. Finite element contact interfaces adopted for the analysis.

Longitudinal Bond: Mechanical interlock and static friction along the dowel length were modeled using elastic springs positioned along four diametrically opposite lines of the dowel [35].

Transverse Interaction: Bearing stresses, normal contact, and Coulomb friction were represented with surface-to-surface contact elements [35]. Initial contact pressure was applied via a minor thermal expansion. For epoxy-coated dowels, a friction coefficient of 0.05 and a uniform clearance of 0.012 mm were used [35].

2.3.3 Mesh Development

Eight-node C3D8R elements were used with aspect ratios below 2. Mesh refinement was applied in critical zones, including dowel holes and load areas, to accurately capture stress gradients [53]. The mesh-sensitivity results presented in Table 3 confirmed less than 1.3 % variation in stress, validating numerical convergence [37]. Figure 3 and Figure 4 show the finite element mesh and the meshed dowel bar, respectively.

Table 3. Mesh Sensitivity Analysis

Mesh Type	Number of Elements	Maximum Tensile Stress (Pa)	Execution Time
Mesh I	27,795	2.36×10^6	8 hours
Mesh II	31,873	2.39×10^6	15 hours
Mesh III	41,174	2.37×10^6	1.5 days

Note: Variation < 1.3 %, confirming convergence. Mesh II adopted as optimal.

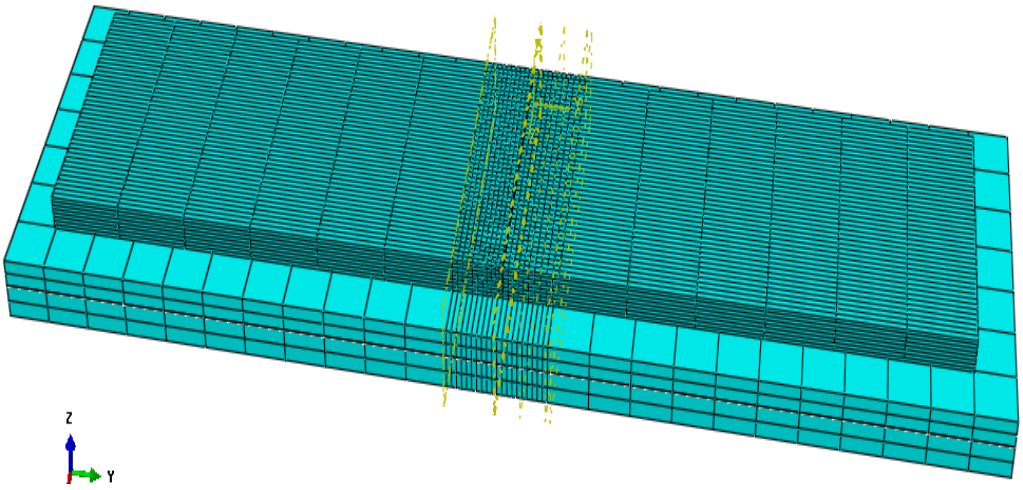

Figure 3. Finite element mesh of a jointed plain concrete pavement (JPCP).

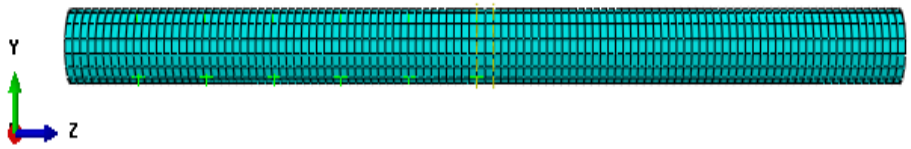

Figure 4. Meshed FE model of a dowel bar

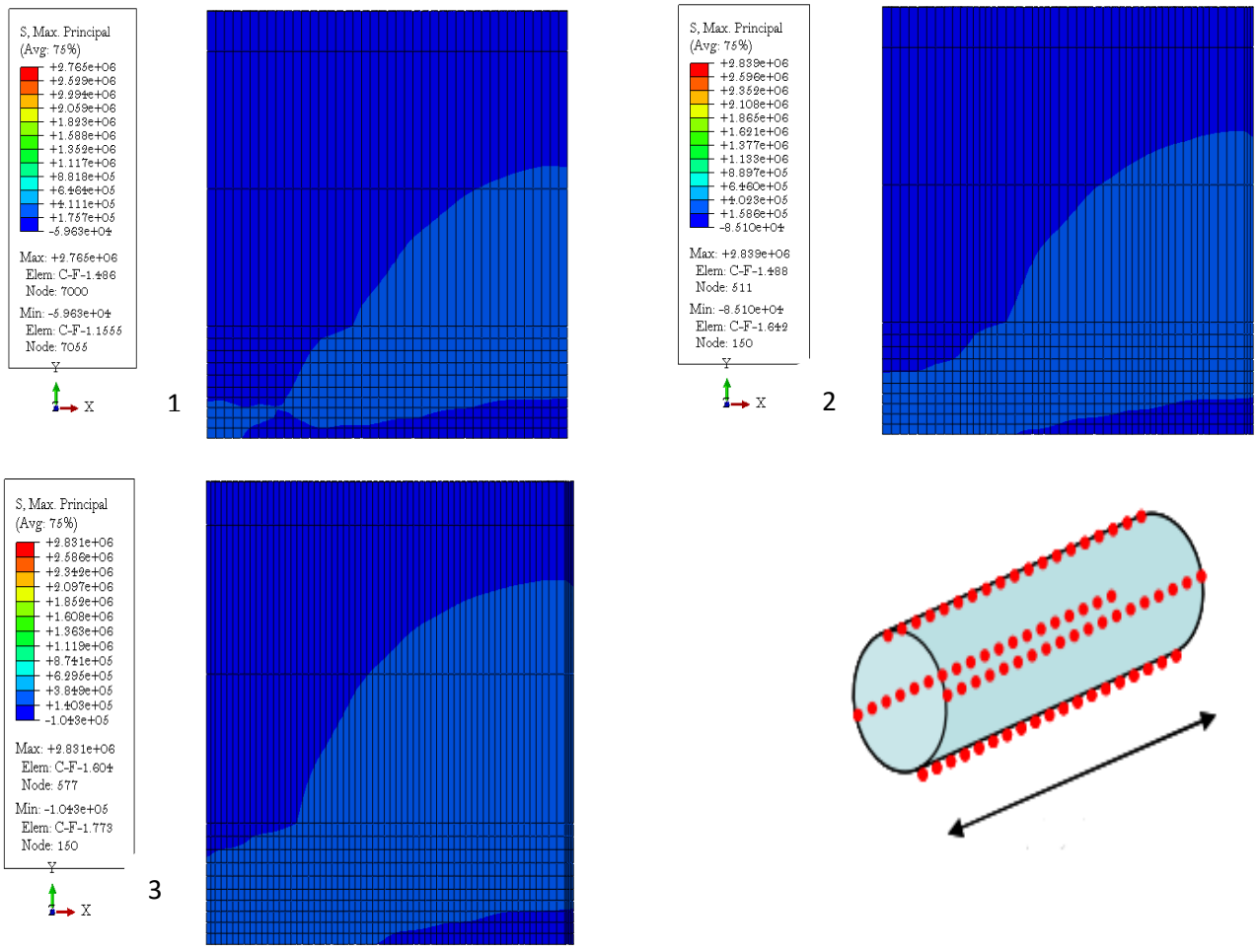

Figure 5. Mesh sensitivity analysis (Meshes 1–3) and the spring-force distribution along half of the dowel [15].

2.3.4. Boundary Conditions

The bottom surface of the subgrade was fully fixed to represent bedrock support [39]. Nodes along the base and subgrade perimeter were horizontally restrained (ux, uy). Slab faces along the longitudinal direction were restrained in x; the transverse joint face was left free, and the opposite slab face was fully constrained in all translational degrees of freedom [54], as illustrated in Figure 6.

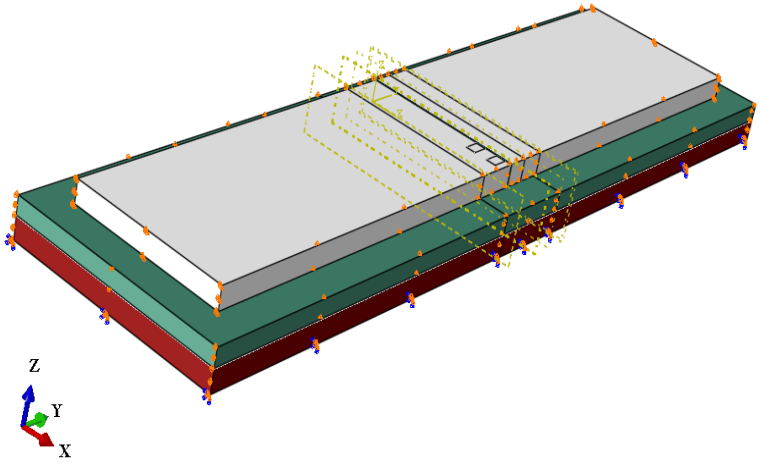

Figure 6. Boundary conditions applied in the finite element (FE) model.

2.3.5. Finite Element Analysis Procedure

Nonlinear 3-D analysis was performed in five stages: one initial step, three static-general steps, and one static Riks step with automatic time increments (initial size 0.001) [37]. The NLGEOM option accounted for large displacements due to geometric, material, and boundary nonlinearities [37]. The first step applied boundary and temperature loads, followed by staged introduction of contact, friction, and wheel load [37], aligning with best practices in nonlinear pavement modeling [15, 35, 37].

2.4. Model Validation

The developed finite-element model (FEM) was validated against Friberg's analytical formulation for dowel deflection and bearing stress [9, 23]. According to the analytical approach, Friberg's closed-form solution is applicable when the parameter $\beta L > 2$, where L represents the dowel embedment length within one slab [9]. In this study, $\beta L = 3.185$, confirming the validity of using Friberg's equation for comparison with the finite-element analysis (FEA) results [9, 23].

Deviations of less than 2.5 % between analytical and numerical results confirmed the model's numerical accuracy and the adequacy of the adopted boundary and contact conditions [9, 23]. Furthermore, the model was evaluated against AASHTO performance criteria [2], consistently predicting load-transfer efficiency (LTE) values above 70 % and relative joint deflections below 0.25 mm [2, 38].

The validation procedure included computations of load transfer, modulus of subgrade reaction, radius of relative stiffness, effective dowel count, and load carried by the critical dowel, following Eqs. (1)–(14) [15, 30, 55]. The model was subjected to a dual-wheel loading configuration, as illustrated in Figure 1, and the resulting FEA outputs were compared with Friberg's closed-form analytical solution for compressive bearing stress [9, 56].

2.4.1. Validation - Load Transfer and Dowel Response

Step 1 — Load Transferred Across the Joint

It is assumed that 45% of the applied wheel load is transferred across the transverse joint:

$$P_t = 0.45\, P_w \quad (1)$$

For an applied wheel load of $P_w = 20$ kN:

$$P_t = 0.45 \times 20 = 9.0 \text{ kN} \quad (2)$$

Step 2 — Modulus of Subgrade Reaction

The modulus of subgrade reaction is determined using the empirical relation:

$$K = \left(\frac{E_{SG}}{20.15}\right)^{0.779} \quad (3)$$

Given $E_{SG} = 310$ MPa $= 44{,}925.2$ psi:

$$K = 405.75 \text{ psi/in} = 109.99 \text{ MPa/m} \quad (4)$$

Step 3 — Radius of Relative Stiffness
The radius of relative stiffness is computed as:

$$l_r = \left(\frac{E_c h^3}{12(1-\mu^2)K \times 19.7}\right)^{0.25} \quad (5)$$

Using the model parameters E_c, h, μ, K, the result obtained is:

$$l_r = 0.7014 \text{ m}$$

Step 4 — Number of Effective Dowels
Dowels located within one radius l_r are considered effective.
For a dowel spacing of $s = 0.30$ m:

$$n = \text{Int}\left(\frac{l_r}{s}\right) + 1 = \text{Int}\left(\frac{0.7014}{0.30}\right) + 1 = 3 \quad (6)$$

Using load distribution coefficients $x_1 = 0.572$ and $x_2 = 0.144$:

$$n_{eff} = 1 + x_1 + x_2 = 1.716 \quad (7)$$

Step 5 — Load on the Critical (Corner) Dowel
The load on the corner dowel is given by:

$$P_{c1} = \frac{P_t}{n_{eff}} = \frac{9.0}{1.716} = 5.24 \text{ kN} \quad (8)$$

Contributions from adjacent dowels are:

$$x_1 P_{c1} = 2.77 \text{ kN}, \quad x_2 P_{c1} = 0.76 \text{ kN} \quad (9)$$

Thus, the total load carried by the corner dowel (including adjacent effects) is approximately:

$$P_{corner,\ total} \approx 8.0 \text{ kN}$$

Step 6 — Dowel Support Stiffness, Analytical Comparison, and Model Validation
From the finite element analysis (FEA):

$$\sigma_{0,FEA} = 7.524 \text{ MPa}, \quad y_{0,FEA} = 0.000165098 \text{ m} \quad (10)$$

The corresponding dowel support stiffness is:

$$K = \frac{\sigma_0}{y_0} = \frac{7.524}{0.000165098} = 4.557 \times 10^{10} \text{ N/m}^3 \quad (11)$$

The relative dowel stiffness is:

$$\beta = \left(\frac{Kd^4}{4E_d I_d}\right)^{0.25} = 13.74 \text{ m}^{-1} \quad (12)$$

Using Friberg's analytical closed-form solution for identical conditions:

$$y_{0,Analytical} = 0.000161568 \text{ m}, \quad \sigma_{0,Analytical} = 7.363 \text{ MPa} \quad (13)$$

Table 4. Comparison of Dowel Deflection and Stress: FEA vs. Friberg Analytical Solution

Quantity	FEA	Analytical	Absolute Difference	Relative Difference
y_0 (m)	0.000165098	0.000161568	3.53×10^{-6}	2.14%
σ_0 (MPa)	7.524	7.363	0.161	2.14%

Friberg's analytical solution and the finite element model exhibit excellent agreement. The maximum dowel deflection and peak bearing stress deviate by only ≈2.14%, confirming the high numerical accuracy of the developed model and validating the boundary conditions, contact definitions, and dowel–subgrade interaction assumptions for the studied configuration.

2.5. LTE Computation

Deflection-based LTE is computed using the standard formula:

$$\text{LTE (\%)} = \frac{\delta_{loaded}}{\delta_{unloaded}} \times 100 \quad (14)$$

Where δloaded and δunloaded are the maximum deflections of the loaded and adjacent slabs, respectively [11,14,57].

3. RESULTS AND DISCUSSION

3.1 Geometric Parameters

Figure 7 illustrates the influence of transverse joint geometric characteristics on load transfer efficiency (LTE). Increasing slab thickness (CC) from 0.25 m to 0.35 m enhanced LTE by approximately 0.7 %, while increasing dowel diameter (DD) from 32 mm to 38 mm produced a more pronounced improvement of 2.56 %. Conversely, widening the joint width (JW) from 8 mm to 12 mm reduced LTE by 1.24 %. Although these numerical variations appear modest, they emphasize the sensitivity of load transfer performance to geometric configuration.

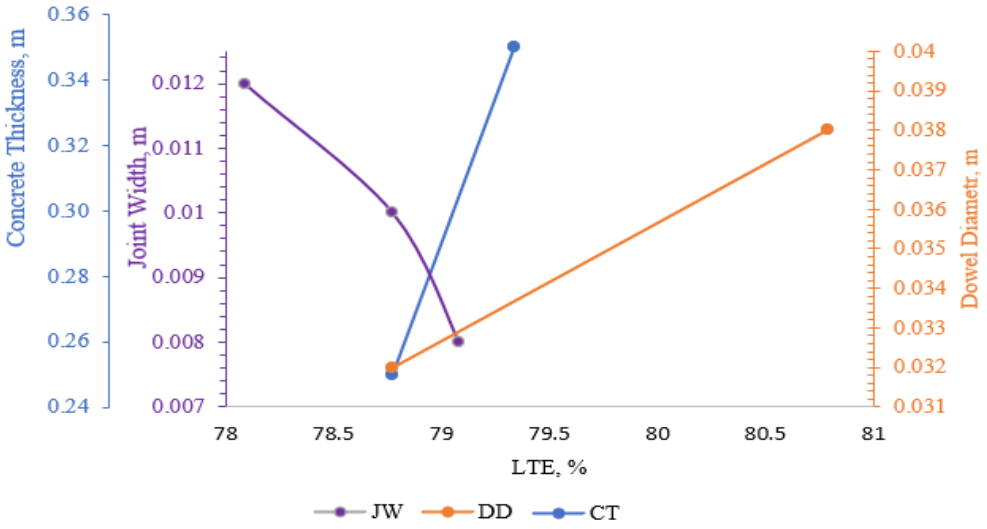

Figure 7. Influence of transverse joint geometric features on load transfer efficiency (LTE).

The deflection-based LTE values were derived from the relative deflections of the loaded and unloaded slabs under combined loading and boundary conditions. The deflection contour for this case is presented in Figure 10.

Overall, geometric parameters must be carefully optimized to balance thermal movement and load transfer efficiency, ensuring long-term pavement performance and minimizing joint distress.

3.2. Traffic and Substructure Parameters

Traffic loading and substructure stiffness represented by axle load and base modulus strongly affect the pavement's load distribution and structural response. The axle load defines the magnitude of traffic-induced stresses, whereas the base modulus quantifies the support provided by the underlying layers.

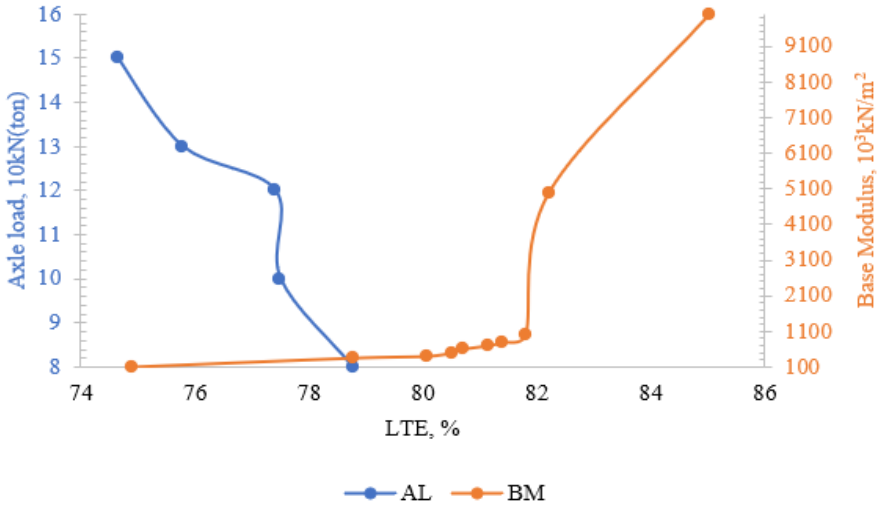

Figure 8. Influence of base modulus and axle load on LTE.

As shown in Figure 8, increasing the base modulus (BM) from 100 MPa to 10 000 MPa resulted in a substantial 13.5 % increase in LTE, indicating that a stiffer base effectively reduces slab deflection and differential joint movement, thereby enhancing load transfer. Conversely, increasing axle load (AL) from 8 tons to 15 tons caused an approximate 4.12 % decrease in LTE, reflecting the amplified deflections and joint movements associated with heavier traffic loads. These findings highlight the importance of using adequately stabilized bases to ensure effective joint performance. For pavements subjected to high traffic loads, design enhancements such as increased slab thickness, higher base stiffness, or larger dowel diameters may be necessary to maintain satisfactory LTE values [7, 8].

3.3. Dowel–Concrete Contact Features

The mechanical interaction between dowel bars and surrounding concrete—characterized by the dowel–concrete friction coefficient and the modulus of dowel support—plays a vital role in local load transfer mechanisms and joint durability. These parameters influence dowel deflection, bearing stress, and long-term performance of the joint.

As illustrated in Figure 9, increasing the modulus of dowel support (MDS) from 1×10^8 kN/m³ to 6×10^8 kN/m³ resulted in a modest 0.4 % increase in LTE. Similarly, varying the dowel–concrete friction coefficient (DCF) between 0.05 and 1.0 altered LTE by less than 1 %. Such small fluctuations fall within computational uncertainty and confirm the model's numerical stability [9, 10].

These results indicate that, while dowel–concrete interface parameters influence localized stress transfer, their overall effect on LTE is minor compared with geometric and substructure stiffness parameters.

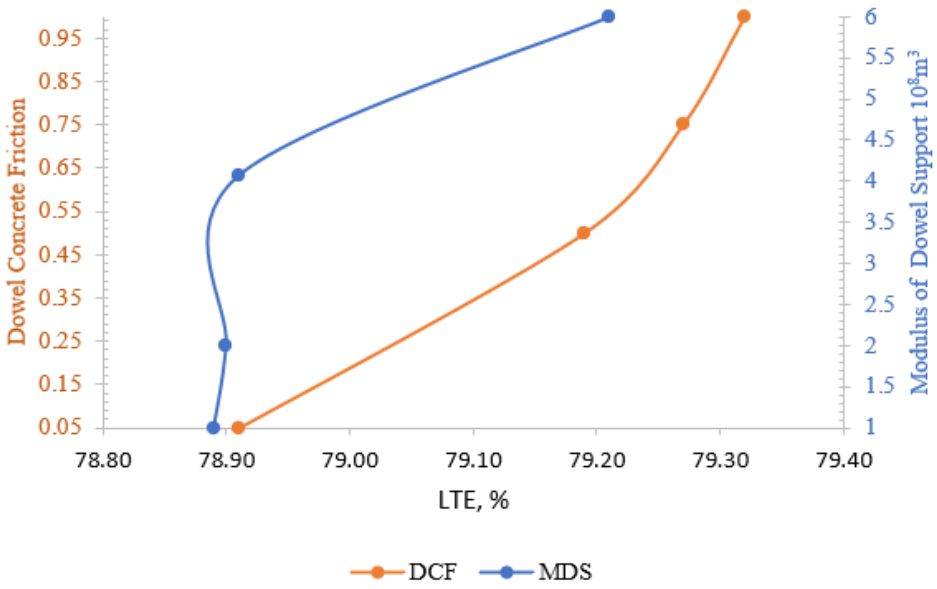

Figure 9. Influence of dowel–concrete contact features on LTE.

A contour plot of the vertical deflection field obtained from the finite element simulation is presented in Figure 10, illustrating representative displacement patterns under dual-wheel loading. This visualization highlights the differential deflection between the loaded and unloaded slabs and supports the observed LTE trends.

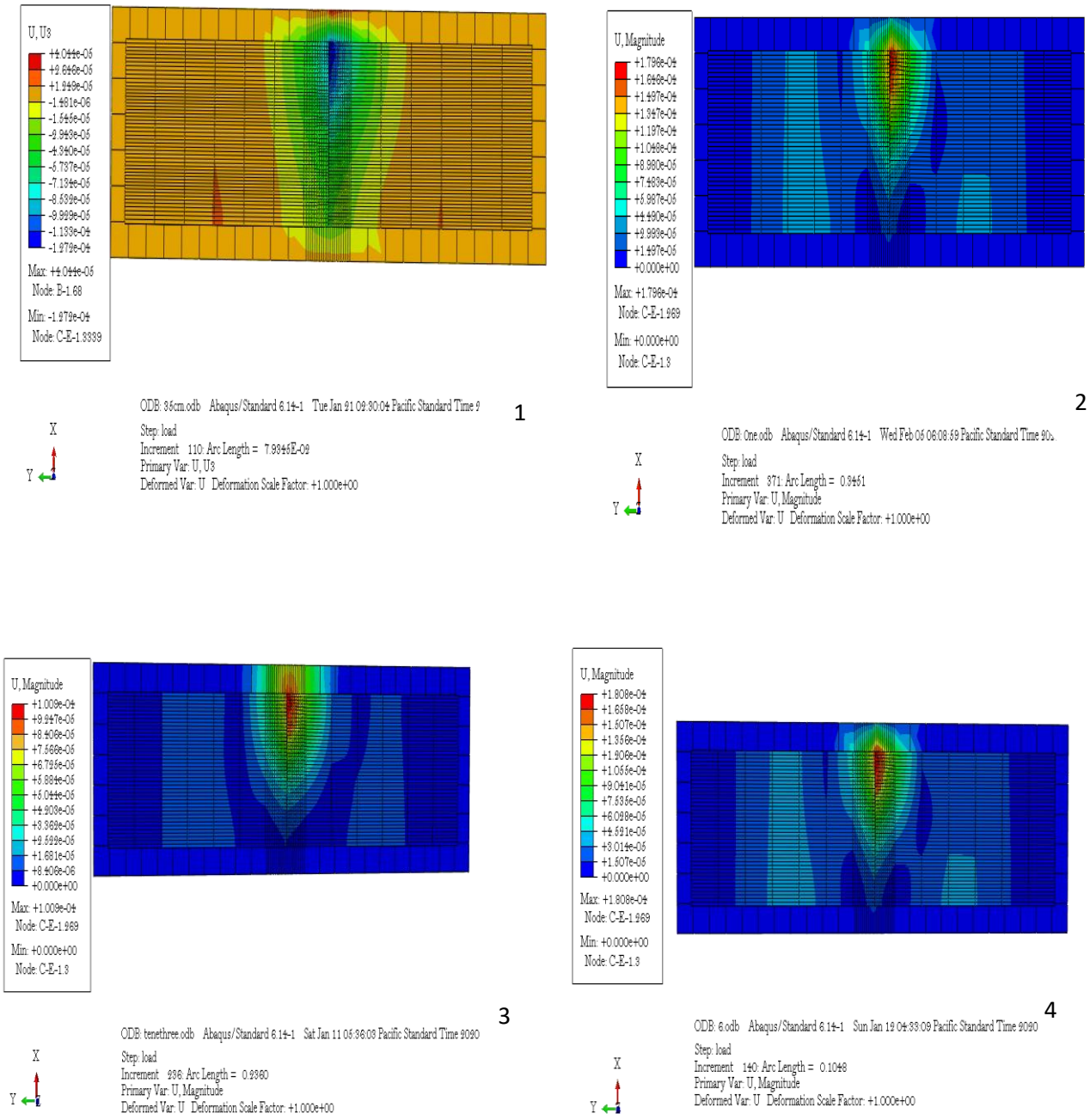

Figure 10. Deflection contour illustrating displacement field for slab (concrete) thickness= 0.35m(1), dowel–concrete friction =1 (2), base modulus = 10,000 MPa/m^2 (3), modulus of dowel support =6 × 10^8 kN/m^3 (4).

4. CONCLUSION

A three-dimensional nonlinear finite element (FE) model was developed to evaluate load transfer efficiency (LTE) in jointed plain concrete pavements (JPCPs). Incorporating the Concrete Damage Plasticity (CDP) model and explicit dowel–concrete contact in Abaqus, the framework accurately simulated realistic joint behavior under dual-wheel loading.

Validation against Friberg's analytical solution showed deviations below 2.5 %, confirming the model's reliability. Predicted LTE values consistently exceeded 70 %, aligning with AASHTO performance thresholds.

Parametric analysis revealed that slab thickness, dowel diameter, and base stiffness significantly enhance LTE, while wider joints and heavier axle loads reduce it. Dowel–concrete interface properties had minimal influence, indicating that geometric and stiffness parameters govern joint performance.

Overall, the developed model offers a robust and efficient tool for mechanistic LTE evaluation, supporting optimized and sustainable JPCP design. Future research should integrate temperature, moisture, and cyclic loading effects for broader applicability.

FUNDING/SUPPORT

This research was fully supported by the Ethiopian Road Authority through the ERA Postgraduate Studies program.

ACKNOWLEDGMENT

The authors gratefully acknowledge the support of the Road and Transport Department at the School of Civil Engineering, Mekelle University.

AUTHORS CONTRIBUTION

This work was carried out in collaboration among all authors.

CONFLICT OF INTEREST

The author (s) declared no potential conflicts of interests with respect to the authorship and/or publication of this paper.

5. REFERENCES

[1] Tan Q, Zhu H, Yang S, Yang X, Ou L. Precast assembled road paving technology: progress and prospects. Materials. 2024;17:2245. [View at Google Scholar]; [View at Publisher]

[2] Owusu-Antwi EB, Meyer AH, Hudson WR. Assessing load transfer across joints and cracks in rigid pavements using the falling weight deflectometer. Research Report No. 460-2. Center for Transportation Research, The University of Texas at Austin; 1990. [View at Google Scholar]; [View at Publisher]

[3] U.S. Department of Transportation, Federal Highway Administration. Evaluation of joint and crack load transfer: final report. FHWA-RD-02-088; 2003. [View at Google Scholar]; [View at Publisher]

[4] Federal Highway Administration. Concrete pavement joints. 2004. [View at Publisher]

[5] Maitra S, Reddy A, Ramachandra R. Load transfer characteristics of dowel bar system in jointed concrete pavement. 2009. [View at Google Scholar]; [View at Publisher]

[6] Yaqoob S, Silfwerbrand J. Assessing the effectiveness of dowel bars in jointed plain concrete pavements using finite-element analysis. Materials. 2025;18(3):588. [View at Google Scholar]; [View at Publisher]

[7] Colley BE, Humphrey HA. Aggregate interlock at joints in concrete pavements. In: Highway Research Record. No. 189. 1967. p. 1–18. [View at Google Scholar]; [View at Publisher]

[8] Colley BE, Humphrey DN. Experimental study of load transfer across concrete pavement joints. Highway Research Record. No. 189. 1967. [View at Google Scholar]; [View at Publisher]

[9] Jayasinghe T, Gunawardena T, Mendis P. Aggregate interlock in fractured concrete mesoscale models: a novel finite element modelling approach. Arch Civil Mech Eng. 2022;22(4):165. [View at Google Scholar]; [View at Publisher]

[10] CesarA Pradena P. Load transfer characterization for the structural design of thinner concrete pavements. Sustainability. 2020;12(21):9153. [View at Google Scholar]; [View at Publisher]

[11] Talebi Jouybari S, Shafabakhsh GA. Finite element investigation of load transfer efficiency in jointed plain concrete pavements. Comput Res Prog Appl Sci Eng. 2017;3(2):91–96. [View at Google Scholar]; [View at Publisher]

[12] Zeng M, Zhao H, Peng K, Bian Z, Wu D. Load transfer efficiency assessment of concrete pavement joints using distributed optical vibration sensor. Appl Sci. 2022;12(18):9273. [View at Google Scholar]; [View at Publisher]

[13] Zhu G, Dong Z, Yang Y, Wang J. Analysis of joint load transfer performance of prefabricated steel–concrete hollow pavement slab. J China & Foreign Highway. 2025;45(1):73–79. [View at Google Scholar]; [View at Publisher]

[14] Friberg BF. Design of dowels in transverse joints of concrete pavements. Trans ASCE. 1940;105(1):1076–1095. [View at Google Scholar]; [View at Publisher]

[15] Zewdie EA, Fujiyama C, Maekawa K. Dowel bar contribution to bond deterioration under cyclic loading. ACI Struct J. 2024;121(5):123–132. [View at Google Scholar]; [View at Publisher]

[16] Nie X, Huang D, Liu T, Fan J. Experimental study on shear transfer across interfaces with post-installed shear reinforcement. J Build Eng. 2024;97:110812. [View at Google Scholar]; [View at Publisher]

[17] Pejatović M, Muttoni A. Experimental investigation of dowel action in reinforcing bars. Struct Concr. 2024;25(7):2732–2758. [View at Google Scholar]; [View at Publisher]

[18] Ghauch ZG. Finite element investigation of deterioration of doweled rigid pavements. 2011. [View at Google Scholar]; [View at Publisher]

[19] Sii HB, Chai GW, van Staden R, Guan H. Effect of dowel looseness on response of jointed concrete pavements using 3D FE analysis. Adv Mater Res. 2014;900:435–444. [View at Google Scholar]; [View at Publisher]

[20] Fasil M, Rahman MK, Al Zahrani MM, Nanni A, Najamuddin SK. Load transfer of small diameter GFRP and stainless steel doweled joints. Eng Struct. 2024;302:117241. [View at Google Scholar]; [View at Publisher]

[21] Li LK, Tan YQ, Gong XB, Li YL. Load transfer characteristics and durability of GFRP dowels in jointed concrete pavement. Adv Eng Forum. 2012;5:277–282. [View at Google Scholar]; [View at Publisher]

[22] Vijay PV, Li H, GangaRao HV. Design and evaluation of JPCP with FRP dowels. FHWA-HRT-06-106; 2009. [View at Google Scholar]; [View at Publisher]

[23] Vijay PV, Li H, GangaRao HV. Decade-long performance evaluation of JPCP with FRP dowels. Int J Pavement Eng. 2020;21(6):713–724. [View at Google Scholar]; [View at Publisher]

[24] Pirdavani A, Bollen T, Ools S, Verheyen S. Optimization of geometry and material properties in JPCP. Transp Res Procedia. 2025;38:124–132. [View at Google Scholar]; [View at Publisher]

[25] Grosek J, Zuzulova A, Brezina I. Effectiveness of dowels in concrete pavement. Materials. 2019;12(10):1669. [View at Google Scholar]; [View at Publisher]

[26] Chen CH, Marshek KM, Saraf CL. Effect of truck tire contact pressure distribution on flexible pavement design. Transp Res Rec. 1986;1095:72–78. [View at Google Scholar]; [View at Publisher]

[27] Chen WF, Han DJ. Plasticity for Structural Engineers. Gau Lih Book Co. Ltd.; 1995. [View at Google Scholar]; [View at Publisher]

[28] Shoukry SN, William GW, Riad M. Application of LS-DYNA identifying critical stresses around dowel bars. 2011. [View at Google Scholar]; [View at Publisher]

[29] Shoukry SN, William GW, Riad M. Effect of dowel bar looseness on measured LTE using FWD. 2001. [View at Google Scholar]; [View at Publisher]

[30] Shoukry SN, Fahmy M, Prucz J, William G. Validation of 3D FE analysis of rigid pavement dynamic response. Int J Geomech. 2007;7(1):16–24. [View at Google Scholar]; [View at Publisher]

[31] Keymanesh MR, Babaki MM, Shahriari N, Pirhadi A. Evaluating dowel performance in PCC pavement using ABAQUS. Int J Transp Eng. 2018;5(4):349–365. [View at Google Scholar]; [View at Publisher]

[32] Lubliner J, Oliver J, Oller S, Onate E. A plastic-damage model for concrete. Int J Solids Struct. 1989;25:299–326. [View at Google Scholar]; [View at Publisher]

[33] Lee J, Fenves GL. Plastic-damage model for cyclic loading of concrete structures. J Eng Mech. 1998;124(8):892–900. [View at Google Scholar]; [View at Publisher]

[34] Bilal KA, Mahamid M, Hariri-Ardebili MA, Tort C, Ford T. Parameter selection for concrete constitutive models. Buildings. 2023;13(7):1759. [View at Google Scholar]; [View at Publisher]

[35] Mathern A, Yang J. Practical FE modelling strategy for cracking and crushing behavior of RC structures. Materials. 2021;14:506. [View at Google Scholar]; [View at Publisher]

[36] Azadravesh E. Generating a 3D model for evaluating joint opening effects in concrete pavements using ABAQUS. 2010. [View at Google Scholar]; [View at Publisher]

[37] Gillespie TD, et al. Effects of heavy vehicle characteristics on pavement response and performance. NCHRP Final Report; 1992. [View at Google Scholar]; [View at Publisher]

[38] Khazanovich L, Buch N, Gotlif A. Evaluation of alignment tolerances for dowel bars. Michigan DOT; 2001. [View at Google Scholar]; [View at Publisher]

[39] Chua BT, Nepal KP. Review of performance criteria and key design parameters for JPCP. Am J Civ Eng. 2025;13(3):165–184. [View at Publisher]

[40] Rahman MT, Mahmud K, Ahsan S. Stress–strain characteristics of flexible pavement using FE analysis. Int J Civil Struct Eng. 2011;2(1):233–240. [View at Google Scholar]; [View at Publisher]

[41] ABAQUS. Version 6.14. Dassault Systèmes; 2014. [View at Google Scholar]; [View at Publisher]

[42] Sadeghi V, Hesami S. Investigation of LTE in JPCP using FEM. Int J Pavement Res Technol. 2018;11:245–252. [View at Google Scholar]; [View at Publisher]

[43] Alzamily A, Al-Jelawy HM, Jashami H. FE simulation of shear stud JPCP utilizing UHPC link slabs. Discover Civil Eng. 2025;2:Article 43. [View at Google Scholar]; [View at Publisher]

[44] Luoke L, Yiqiu T, Xiangbing G, Yunliang L. Characterization of contact stresses between dowels and concrete. Int J Civil Environ Eng. 2012;12(5):23–27. [View at Google Scholar]; [View at Publisher]

[45] Lévy C. FE analysis of jointed concrete pavements: load transfer mechanisms. PhD thesis. Université de Sherbrooke; 2010. [View at Publisher]

[46] Mackiewicz P. Analysis of stresses in pavement under a dowel. Can J Civ Eng. 2015;42(11):845–853. [View at Google Scholar]; [View at Publisher]

[47] Friberg BF. Load and deflection characteristics of dowels in pavement joints. Proc Highway Res Board. 1938;18:140–154.

[48] Lubliner J, Oliver J, Oller S, Onate E. A plastic-damage model for concrete. Int J Solids Struct. 1989;25:299–326. [View at Google Scholar]; [View at Publisher]

[49] Timoshenko S, Lessels JM. Applied Elasticity. 1925. p. 133–141. [View at Google Scholar]; [View at Publisher]

[50] Albertson MD. Fiber composite and steel pavement dowels. Master's thesis. Iowa State University; 1992. [View at Google Scholar]; [View at Publisher]

[51] American Association of State Highway and Transportation Officials. AASHTO Guide for Design of Pavement Structures. 1993. [View at Google Scholar]; [View at Publisher]

[52] Sadeghi V, Hesami S. Investigation of LTE in JPCP using FEM. Int J Pavement Res Technol. 2018;11:245–252. [View at Google Scholar]; [View at Publisher]

[53] Snyder MB. Improved protocol for structural evaluation of dowel load transfer systems. Iowa State University; 2021.

[54] Jagadeesh A, Premarathna WAAS, Kumar A, Kasbergen C, Erkens SMJG. FE modelling of JPCP under rolling forklift tire. Eng Struct. 2025;328:119705. [View at Google Scholar]; [View at Publisher]

[55] Yaqoob S, Silfwerbrand J, Balieu RGR. Parametric study on dowel LTE using FE modelling. Buildings. 2024;14(4):1039. [View at Google Scholar]; [View at Publisher]

[56] Elseifi MA, Baek J, Dhakal N. Review of modelling crack initiation/propagation in flexible pavements. Int J Pavement Eng. 2018;19(3):251–263. [View at Google Scholar]; [View at Publisher]

[57] Hua J. FE modeling and analysis of accelerated pavement testing devices. PhD thesis. Purdue University; 2000. [View at Google Scholar]; [View at Publisher]